

Article

Transcriptome Analysis of Egg Yolk Sialoglycoprotein on Osteogenic Activity in MC3T3-E1 Cells

Sizhe He^{1,2,3,†}, Keke Meng^{1,2,3,†}, Muxue Chen^{1,2,3,†} , Lehui Zhu^{1,3}, Qingying Xiang^{1,3}, Zhangyan Quan^{1,3}, Guanghua Xia^{1,2,3,4,*}  and Xuanri Shen^{1,2,3,4,*}

- ¹ Hainan Engineering Research Center of Aquatic Resources Efficient Utilization in South China Sea, Hainan University, Haikou 570100, China; 19083200210001@hainanu.edu.cn (S.H.); 19083200210007@hainanu.edu.cn (K.M.); chenmuxue15622156189@hotmail.com (M.C.); 20180881310055@hainanu.edu.cn (L.Z.); 20190881310023@hainanu.edu.cn (Q.X.); 20190881310102@hainanu.edu.cn (Z.Q.)
- ² Collaborative Innovation Center of Marine Food Deep Processing, Dalian Polytechnic University, Liaoning 116000, China
- ³ College of Food Science and Technology, Hainan University, Haikou 570100, China
- ⁴ Key Laboratory of Seafood Processing of Haikou, Haikou 570100, China
- * Correspondence: 993050@hainanu.edu.cn (G.X.); Shenxuanri2009@163.com (X.S.); Tel.: +86-189-7654-3028 (G.X.); +86-135-1889-8909 (X.S.)
- † These authors contributed equally to this study.

Abstract: In this study, the effects of egg yolk sialoglycoprotein (EYG) on osteogenesis in MC3T3-E1 cells were investigated and the DEGs (differentially expressed genes) were explored by transcriptome analysis. The results found that EYG effectively increased cell proliferation, enhanced ALP activity, promoted the secretion of extracellular matrix protein COL-I and OCN, enhanced bone mineralization activity, exhibiting good osteogenic activity. Further study of the mechanism was explored through transcriptome analysis. Transcriptome analysis showed that 123 DEGs were triggered by EYG, of which 78 genes were downregulated and 45 genes were upregulated. GO (gene ontology) analysis showed that EYG mainly caused differences in gene expression of biological processes and cell composition categories in the top 30 most enriched items. KEGG (Kyoto Encyclopedia of Genes and Genomes) analysis showed that EYG inhibited inflammatory factors and downregulated inflammation-related pathways. The results also showed EYG regulated such genes as COL2A1, COL4A1 and COL4A2 to up-regulate pathways including ECM–receptor interaction, focal adhesion and protein digestion and absorption, enhancing the proliferation and differentiation of osteoblasts. Gene expression of COL-I, Runx2, BMP2 and β -catenin was determined by qRT-PCR for verification, which found that EYG significantly increased COL-I, Runx2, BMP2 and β -catenin gene expression, suggesting that BMP-2 mediated osteogenesis pathway was activated.

Keywords: egg yolk; sialoglycoprotein; MC3T3-E1 cells; osteogenesis; transcriptome analysis



Citation: He, S.; Meng, K.; Chen, M.; Zhu, L.; Xiang, Q.; Quan, Z.; Xia, G.; Shen, X. Transcriptome Analysis of Egg Yolk Sialoglycoprotein on Osteogenic Activity in MC3T3-E1 Cells. *Appl. Sci.* **2021**, *11*, 6428. <https://doi.org/10.3390/app11146428>

Academic Editor: António José Madeira Nogueira

Received: 2 June 2021
Accepted: 1 July 2021
Published: 12 July 2021

Publisher's Note: MDPI stays neutral with regard to jurisdictional claims in published maps and institutional affiliations.



Copyright: © 2021 by the authors. Licensee MDPI, Basel, Switzerland. This article is an open access article distributed under the terms and conditions of the Creative Commons Attribution (CC BY) license (<https://creativecommons.org/licenses/by/4.0/>).

1. Introduction

According to the World Health Organization, osteoporosis is defined as a condition in which the standard value of average peak bone mineral density is more than 2.5 standard deviations below that of healthy adults [1]. As a class of metabolic bone diseases characterized by low bone mass and microstructural changes in bone tissue, patients are at higher risk of fracture. It currently afflicts 200 million people worldwide, and is becoming the seventh most common disease [2,3]. Primary osteoporosis is a series of physiological diseases that occur with the increase of age and include postmenopausal osteoporosis, senile osteoporosis and idiopathic osteoporosis. Generally speaking, osteoporosis is more likely to occur in middle age due to imbalance of bone metabolism in the body's bone metabolism. The occurs of osteoporosis is due to the weakened osteoblasts, which are responsible for bone formation, or enhanced osteoclasts, which are responsible for bone

resorption. As the basic functional units of bone formation, osteoblasts are essential for the balance of bone metabolism [4]. Stimulating the proliferation of osteoblasts and promoting their differentiation and maturation is one of the effective methods to prevent and treat osteoporosis. However, the current drugs have serious side effects [5], food-derived anti-osteoporotic functional factors have become a research hotspot due to their safety. A large number of studies have confirmed that food-derived functional factors, such as soy isoflavone [6], fish oil [7], polyphenol [8], saccharides [9,10], peptide [11], exhibited excellent effects on the treatment of osteoporosis.

In vivo, osteoblasts respond to various factors involved in proliferation and differentiation [12]. During differentiation, pre-osteoblasts express extracellular matrix proteins, such as type I collagen (COL-I), alkaline phosphatase (ALP), osteocalcin (OCN), and other bone matrix proteins, which help Ca^{2+} deposition and mineralization [13–15]. Osteogenesis is regulated by some transcription factors and cytokines, such as Runx2, osterix, BMP-2 and β -catenin [16]. Runx2, a transcription factor that has similar Runx2 binding and gene expression profiles in mouse and human osteoblasts, is essential for osteoblast differentiation and bone formation [17]. Activated Runx2 induces the expression of osteoblast-specific genes such as COL-I, ALP, OCN, resulting in osteoblast differentiation and mineralization [18]. Osteoblasts are subject to complex gene regulation during differentiation. As a member of the TGF family, BMP-2 plays a vital role in the regulation of bone formation. It has been proved that BMP-2 can accelerate the specific differentiation of osteoblasts [19]. BMP-2 specifically binds to the receptor and activates phosphorylation of downstream Smad proteins to form a hetero-oligomeric complex with a common mediator Smad, thereby regulating downstream target genes such as Runx2 [20,21]. BMP-2 also interacts with other pathways to regulate osteoblast differentiation. In the osteoblasts lineage, β -catenin can affect osteoblasts and osteoclasts through pathways that increase bone mass [22]. The Wnt/ β -catenin signaling pathway increases bone formation by stimulating osteoblast proliferation, and inhibiting GSK3 activity disrupts the protein complex, resulting in no longer phosphorylated β -catenin [23], thereby activating transcription factor activity for regulation [24]. Besides, GSK-3 β / β -catenin signaling pathway was found to be one of the key downstream pathways of the PI3K/AKT pathway, which regulates bone formation [23]. It has been found that PI3K/AKT increased phosphorylation of GSK-3 β in murine osteoblastic MC3T3-E1 cells, leading to β -catenin stabilization and β -catenin-mediated transcription, which indicated that the PI3K/AKT/ β -catenin axis is functional in regulating osteoblasts [25].

Eggs from hens are considered to be a traditional food rich in a variety of bioactive ingredients, including polyunsaturated fatty acids, immunoglobulin, lecithin, and others [2,26]. Recently, some studies have indicated that the sialoglycoprotein of crucian carp egg can show good anti-osteoporosis ability in vivo and in vitro [27,28]. A lot of research has been done on the extraction of sialoglycoprotein from egg yolk [29,30]. There is a study finding that the bone marker serum bone alkaline phosphatase (BALP) was significantly increased after feeding the egg hydrolysate in orchietomized dogs [31]. Egg yolk protein from hen eggs could significantly improve bone growth rate and expression of BMP-2 in adolescent male rats [32]. Besides, egg yolk soluble protein from hen eggs promoted the proliferation and differentiation of osteoblastic MC3T3-E1 cells [33]. It has been found that the yolk-derived functional factor from hen eggs has a protective effect on bone metabolism and has a potential effect on the prevention of osteoporosis both in MC3T3-E1 cells and ovariectomized rats [26]. However, there is still a lack of research on the effective factors and mechanisms of osteogenic activity in egg yolk extract.

On that basis, we explored the effects of egg yolk sialoglycoprotein (EYG) on proliferation, differentiation and mineralization in MC3T3-E1 cells, and investigated the osteogenic mechanism by transcriptome analysis. The study provided several enriched DEGs (differentially expressed genes) and pathways for future research into the molecular mechanisms of bone formation.

2. Materials and Methods

2.1. Materials and Regents

ALP reagent kits and BCA were obtained from Beyotime Institute of Biotechnology. COL-I and OCN ELISA kits were purchased from Nanjing Jiancheng Bioengineering Research Institute. α -MEM medium, fetal bovine serum (FBS), penicillin and streptomycin were obtained from ThermoFisher Biochemical Products Co., Ltd. L-ascorbic acid, β -sodium glycerophosphate cetylpyridine chloride and MTT were purchased from Sigma-Aldrich. HCHO was produced by Guangzhou Chemical Reagent Factory.

2.2. Preparation of EYG

EYG was prepared according to the method of Sun and Liu et al. [34,35]. All preparation procedures were operated at 4 °C. Eggs yolk from wenchang chicken (500 g) was homogenized in isopycnic 0.5 M NaCl for 5 min, and then mixed with 90% phenol ($v/v = 5:1$) and the mixture was stirred for 30 min. After centrifugation at $10,000 \times g$ for 20 min, the aqueous phase was decanted into a dialysis bags with 2000 Da sectional molecular weight, dialyzed against tap water for 3 days, then against distilled water for 1 day to remove the phenol. The crude glycoprotein was then lyophilized and applied to a column (2.6×50 cm) of DEAE-52 (preequilibrated with 0.01 M Tris-HCl buffer, pH 8.0), eluted with a linear gradient of NaCl (0–1 M) in 0.02 M Tris-HCl buffer. The elution profile was monitored by the absorbance at 280 nm for protein, and the phenol-sufuric acid method for hexose. Protein-positive and hexose-positive overlapping fraction were collected and applied to a Sephadex G-50 (2.0×100 cm, equilibrated and eluted with 0.1 M NaCl), the profile was monitored according to the above methods. After isolation with Sephadex G-50, a single overlapping peak of protein and hexose was obtained, lyophilized and designated as EYG. Its purity is 94.57% measured with HPLC, and molecular weight was 28.045 kDa measured with MALDI-TOF/TOF.

2.3. Cell Culture

Pre-osteoblast MC3T3-E1 cells were cultured in α -MEM medium supplemented with 10% fetal bovine serum, 100 U/mL penicillin and streptomycin in an incubator at 37 °C with 5% carbon dioxide and 95% air humidity. MTT method is used for determination of MC3T3-E1 cells' proliferation activity and the MC3T3-E1 cells were purchased from ATCC (American Type Culture Collection).

2.4. Determination of Proliferative Activity

To determine the proliferative activity in MC3T3-E1 cells, cells (2×10^4 each well) were seeded into 96-well plates and then modified with medium containing EYG (0, 6.25, 12.5, 25, 50, 100 $\mu\text{g/mL}$). After culture for 48 h, the absorbance of each well was determined by MTT method, and its absorbance value was measured at $A_{490 \text{ nm}}$.

2.5. ALP Activity Assay

To evaluate the ALP activity in MC3T3-E1 cells, cells (2×10^4 each well) were seeded into 96-well plates and then modified with EYG-treated (0, 6.25, 12.5, 25, 50, 100 $\mu\text{g/mL}$) osteogenic differentiation medium (10 mM β -sodium glycerophosphate, 50 $\mu\text{g/mL}$ L-ascorbic acid, 10% FBS, 100 U/mL streptomycin-penicillin). The culture medium was changed every other day. After culture for 7 days, the cells were washed with phosphate-buffered saline (PBS) twice and lysed with 300 μL 1% Triton X-100 lysis buffer for 20 min. The supernatant was collected by centrifuging at $12,000 \times g$, an ALP reagent kit was used to measure the supernatant ALP activity levels (U/mL) and a BCA detection kit was used to measure the total amount of cell protein.

2.6. Determination of COL-I and OCN Content

To determine the supernatant content of COL-I on day 7 and OCN on day 14 secreted by MC3T3-E1 cells, cells (2×10^4 each well) were seeded into 96-well plates and then

modified with EYG-treated α -MEM medium (0, 6.25, 12.5, 25, 50, 100 $\mu\text{g}/\text{mL}$). The cell supernatant was collected on day 7 and day 14, respectively. The COL-I and OCN content in MC3T3-E1 cells were detected according to the instructions of ELISA kits.

2.7. Alizarin Red Staining Assay

Alizarin red staining assay was performed to determine the formation of mineralized matrix nodules. After 17 days of culture, the supernatant was removed, the cells were washed with PBS twice, fixed with 300 μL 4% neutral formaldehyde for 15 min, and then washed with PBS twice. Finally, after the cells were stained with 1% alizarin red solution for 30 min in a dark condition at 37 $^{\circ}\text{C}$, the cells were cleaned with distilled water 3 times, observed and photographed.

Cetylpyridine chloride was added at 37 $^{\circ}\text{C}$ (300 μL) at a concentration of 100 mM for 15 min. A supernatant of 300 μL was taken for semi-quantitative detection, and the absorbance was recorded at a wavelength of 570 nm using a microplate reader.

2.8. RNA-seq

The cells (2×10^4 each well) were seeded into 96-well plates and then modified with EYG-treated (0, 50 $\mu\text{g}/\text{mL}$) α -MEM medium with 10 mM β -sodium glycerophosphate, 50 $\mu\text{g}/\text{mL}$ L-ascorbic acid, 10% FBS, 100 U/mL streptomycin-penicillin. The culture medium was changed every other day, and then the cells were collected on day 7. The purity of RNA was measured by Nanodrop 2000. We quantified RNA concentration accurately using Qubit and detected RNA integrity using Agilent 2100. The next steps were to construct the library, including mRNA enrichment, double-stranded cDNA synthesis, terminal repair plus A and connector, fragment selection, and PCR enrichment.

In RNA-seq analysis, we estimated the expression level of a gene by counting the sequences (reads) that were localized to the genomic region or the exon region of the gene. FPKM (expected number of Fragments Per Kilobase of transcript sequence per Millions base pairs Sequenced) is the most commonly used method for gene expression level estimation. HTSEQ software was used to analyze the gene expression level of each sample, and the model was UNION. R package was used for GO enrichment analysis, and Goseq was used for enrichment, which based on Wallenius non-central hyper-geometric distribution. We performed the GO analysis with all DEGs including upregulated and downregulated DEGs. The scatter plot was a graphical display of the results of KEGG enrichment analysis, and the KEGG enrichment degree was measured by the Rich Factor, Qvalue and the number of genes enriched in this pathway. As for PPI, BlastX was applied to compare the sequences in the target gene set to the protein sequences of the reference species contained in the STRING database firstly, then the interaction relationship in the STRING protein interaction database was applied to analyze the differential gene protein interaction network, and imported into the Cytoscape software for visual editing finally.

All RNAseq data was available at the Novogene data platform (<https://magic.novogene.com>, accessed on 15 January 2020).

2.9. qRT-PCR

The cells (2×10^4 each well) were seeded into 96-well plates and then modified with α -MEM medium supplemented with 10% fetal bovine serum, 100 U/mL penicillin and streptomycin, 10 mM β -sodium glycerophosphate, 50 $\mu\text{g}/\text{mL}$ L-ascorbic acid and various concentrations of EYG (0, 6.25, 12.5, 25, 50, 100 $\mu\text{g}/\text{mL}$). The culture medium was changed every other day and cells were collected on days 3, 5 and 7.

The total RNA of cells was extracted using Tiangen Animal total RNA extraction kit purchased from Tiangen Biochemical Technology Co., Ltd. (Beijing, China). All operation followed the manufacturer's instructions. RNA was used to synthesize cDNA with a reverse transcription first chain synthesis kit (Tiangen Biochemical Technology Co., Ltd., Beijing, China). Gene expression levels were investigated by quantitative real-time RT-PCR with the SYBR Green PCR kit (Tiangen Biochemical Technology Co., Ltd., Beijing, China)

and the 20 μL system using 100 ng of first-strand cDNA with the following conditions: 95 °C for 15 min followed by 40 cycles at 95 °C for 10 s, 64 °C for 30 s. The number of cells was 1×10^7 , which was quantified with a cell counter. The concentration of cells used for PCR was consistent in all treatment groups. The relative expression level of genes was expressed as the ratio of target gene expression level and β -actin gene expression level for the data normalization [36]. The primers of genes were as follows in Table 1.

Table 1. Primers used for the real-time polymerase chain reaction (qRT-PCR).

Gene	Sequence (5'-3')
COL-I	F- GACAGGCGAACAAGGTGACAGAG
	R- CAGGAGAACCAGGAGAACCAGGAG
BMP2	F- AAGCGTCAAGCCAAACACAAACAG
	R- GAGGTGCCACGATCCAGTCATTC
RUNX2	F- CGGCAAGATGAGCGACGTGAG
	R- TGCTGCTGCTGCTGCTGTTG
β -CATENIN	F- TGCCGTTCCGCTTCATTATGGAC
β -ACTIN	R- TGGGCAAAGGGCAAGGTTTCG
	F- GTGACGTTGACATCCGTAAGA
	R- GTAACAGTCCGCCTAGAAGCAC

2.10. Statistical Analysis

All data are expressed as the mean \pm standard error. SPSS 25.0 software was used for ANOVA and Duncan's test. A p value of less than 0.05 was considered statistically significant [37].

3. Results

3.1. Effect of EYG on Proliferation of MC3T3-E1 Cells

After the treatment with different concentrations of EYG (0, 6.25, 12.5, 25, 50, 100 $\mu\text{g}/\text{mL}$), the proliferation rate of MC3T3-E1 cells increased in a dose-dependent manner. When the concentration of EYG was 100 $\mu\text{g}/\text{mL}$, the proliferation rate of MC3T3-E1 cells significantly increased to 114.37%, indicating that EYG could significantly promote the proliferation of MC3T3-E1 cells without toxic side effects (Figure 1A).

3.2. Effect of EYG on ALP Activity

ALP is one of the most symbolic biological indicators in osteoblasts and represents the beginning of osteoblast differentiation generally. As a homologous dimer glycoprotein, ALP is synthesized by osteoblasts and releases phosphoric acid into the extracellular matrix, which stimulates the formation of calcium nodules in the extracellular matrix, causes the formation of hydroxyapatite and promotes the maturation and differentiation of osteoblasts [38]. As shown in Figure 1B, with the increasing of EYG concentration, the ALP activity in MC3T3-E1 cells gradually increased and reached its maximum value at EYG concentration of 50 $\mu\text{g}/\text{mL}$, which increased by 144.23%. When the concentration of EYG was 100 $\mu\text{g}/\text{mL}$, the activity of ALP decreased. Compared with the control group, the ALP activities in MC3T3-E1 cells differentiation were significantly increased in EYG groups (Figure 1B).

3.3. Effect of EYG on COL-I and OCN Content

COL-I, as an indicator of early differentiation of osteoblasts, is a prerequisite for bone tissue formation [39]. The net structure formed by COL-I is the basis of mineralization and deposition. With the increase of EYG concentration, the COL-I content secreted by MC3T3-E1 cells also gradually increased. When the EYG concentration was 100 $\mu\text{g}/\text{mL}$,

the COL-I content significantly increased to 8.76 ng/mL, indicating that EYG significantly increased COL-I content (Figure 1D).

OCN is one of the markers of late differentiation of osteoblasts and the main non-collagen extracellular matrix synthesized by osteoblasts specifically. OCN plays an important role in maintaining bone formation and inhibiting abnormal hydroxyapatite crystals [40]. When the concentration of EYG was 50 µg/mL, the content of OCN tended to be stable and the growth rate was 214.53%, indicating that EYG significantly promoted the expression of OCN protein in the late differentiation of MC3T3-E1 cells (Figure 1C).

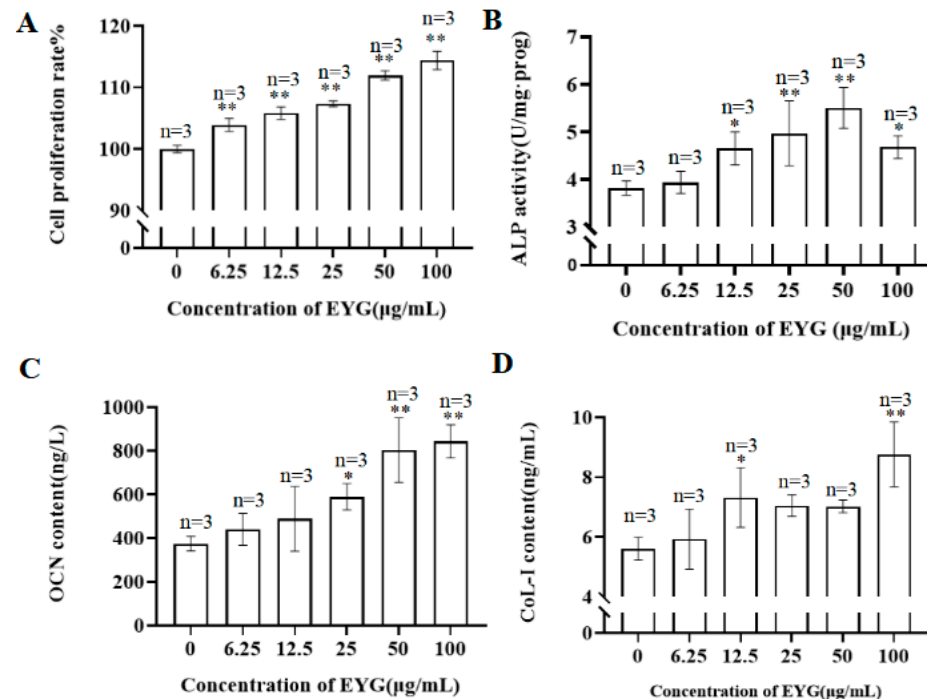


Figure 1. Effect of EYG on cell proliferation (A), cell ALP activity (B), supernatant OCN on day 14 (C) and supernatant COL-I on day 7 (D) content of MC3T3-E1 cells. MC3T3-E1 cells were treated with various concentrations of EYG (0, 6.25, 12.5, 25, 50, 100 µg/mL). Data were expressed as mean ± SEM and the number of replicates was 3 ($n = 3$). Multiple comparisons were done using one way ANOVA analysis. * $p < 0.05$, ** $p < 0.01$ versus control.

3.4. Effect of EYG on Mineralization of MC3T3-E1 Cells

Mineralized bone nodules are the most intuitive manifestation of bone formation, and calcium nodules can specifically bind with alizarin red element to form red chelate complex. As shown in Figure 2A, alizarin red staining showed that with the increasing of EYG concentration, the number of calcium nodules significantly increased with a significant dose-dependent effect.

The calcium nodules were semiquantitatively analyzed by cetylpyridine chloride solution. EYG can significantly promote the mineralization of MC3T3-E1 cells (Figure 2B). Compared with the control group, when the concentration of EYG was 100 µg/mL, there was the most growth rate of calcium nodules, and the growth rate was 199.64%.

3.5. Screening of DEGs

Volcanic plots can be used to infer the overall distribution of differential genes. Genes with similar expression patterns may have similar functions or participate in the same metabolic process or cellular pathway. As shown in Figure 3, compared with control group, the osteoblast MC3T3-E1 detected a total of 123 differentially expressed genes, including 45 upregulated genes and 78 downregulated genes. A genetic volcano plot based on 123 genes revealed the expression profile of these genes in osteoblast MC3T3-E1 cells.

3.6. GO Analysis

GO analysis of DEGs can intuitively reflect the number and distribution of differential gene expression in the GO term enriched in biological processes, cell components and molecular functions. As can be seen in Figure 4, we chose the top 30 most enriched GO items for analysis and the results showed that after treatment with 50 $\mu\text{g}/\text{mL}$ EYG, DEGs in the biological process categories were highly enriched and the pathways included single-organism developmental process, developmental process, anatomical structure development and multicellular organismal development. Pathways including extracellular space and extracellular region were associated with more DEGs in cellular component categories and there were no pathways associated with molecular function categories in the top 30 most enriched items.

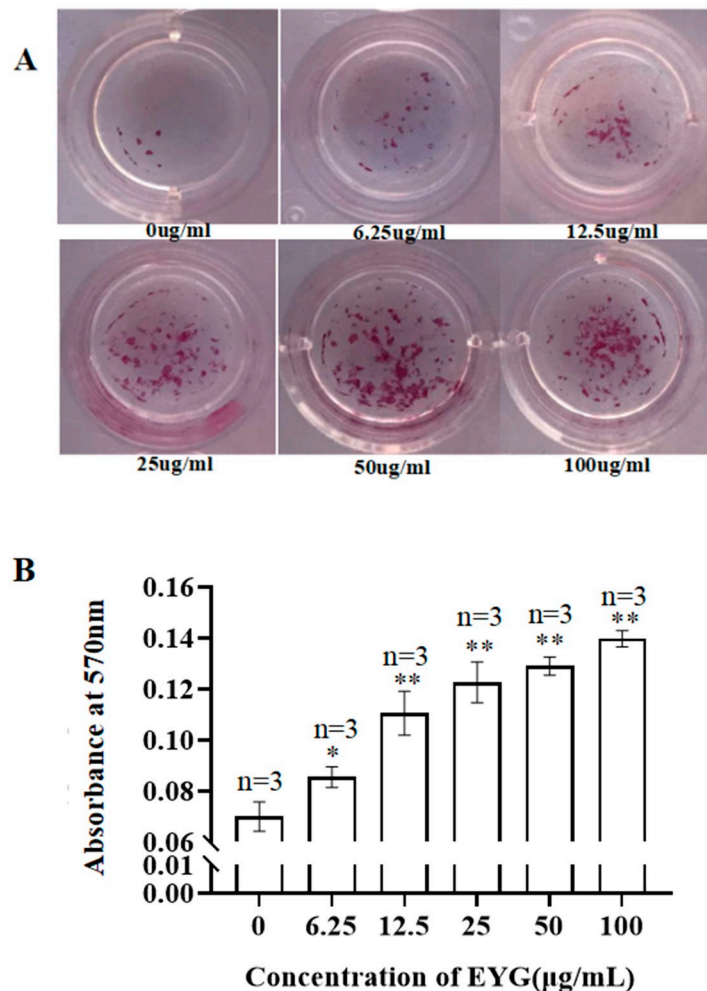


Figure 2. Effect of EYG on mineralized nodular of MC3T3-E1 cells. Morphology (A) and absorbance (B) at 570 nm after staining of MC3T3-E1 cells. MC3T3-E1 cells were treated with various concentrations of EYG. EYG promoted mineralized nodular of MC3T3-E1 cells. Data were expressed as mean \pm SEM and the number of replicates was 3 ($n = 3$). Multiple comparisons were done using one way ANOVA analysis. * $p < 0.05$, ** $p < 0.01$ versus control.

3.7. KEGG Analysis

KEGG enrichment analysis was performed for genes with different expression levels. Scatter plot is a graphical representation of KEGG enrichment analysis results. The 20 pathways with the most significant enrichment were selected (Figure 5). We found that gene expression in several pathways was significantly different after the treatment of EYG

including TNF signaling pathway, complement and coagulation cascades, ECM–receptor interaction, focal adhesion, protein digestion and absorption.

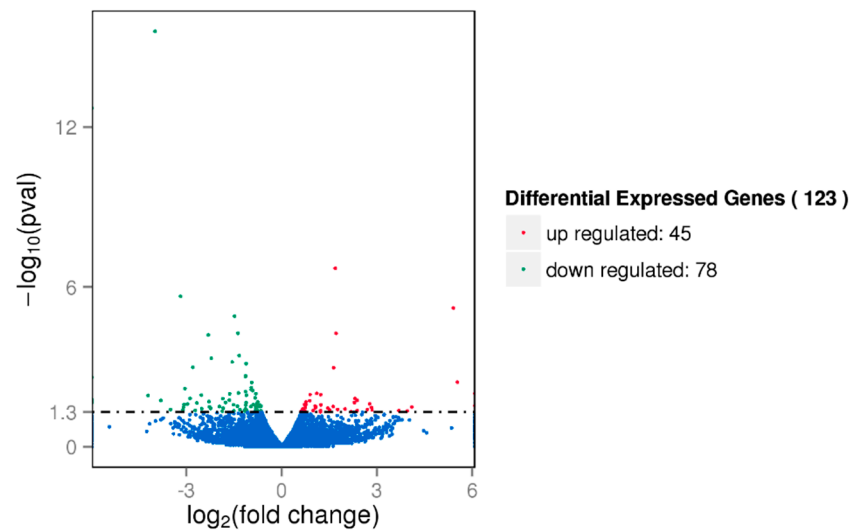


Figure 3. Volcano plot of distribution trends for differentially expressed genes with 50 µg/mL concentrations of EYG and control groups. Each dot represents one gene. Red dots represent upregulated genes and green dots represent downregulated genes. Blue dots represent genes with no differential expression. There are 123 differentially expressed genes in total, including 45 upregulated genes and 78 downregulated genes.

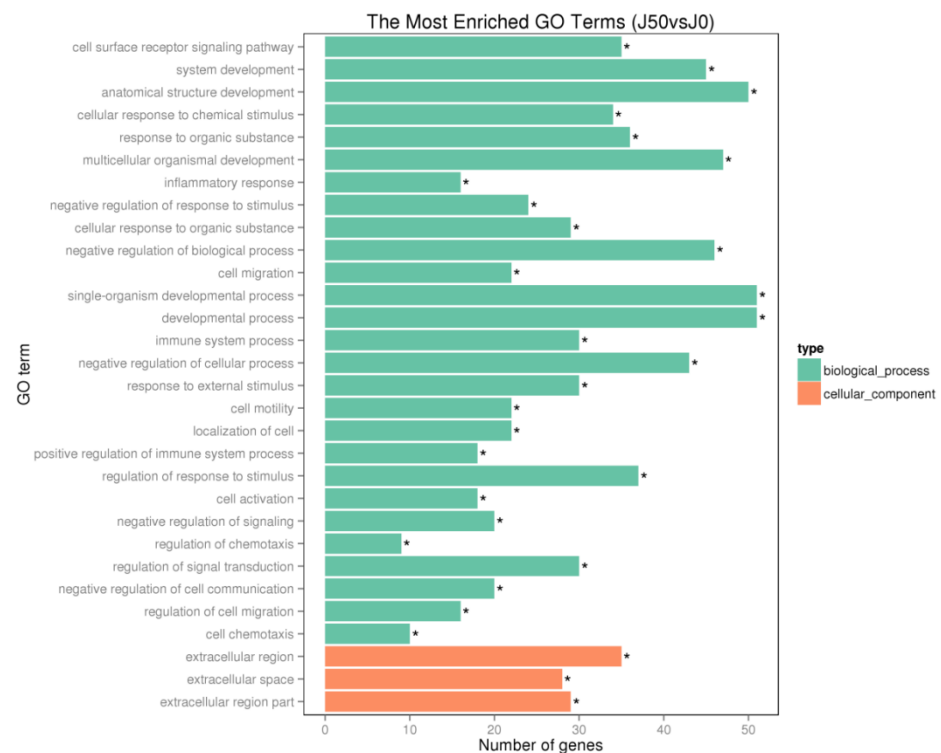


Figure 4. GO analysis of DEGs between 50 µg/mL concentrations of EYG group and control group. The ordinate was the GO term of enrichment, and the abscissa was the number of different genes in the term. Different colors were used to distinguish biological processes, cell components and molecular functions. * GO term was significantly enriched.

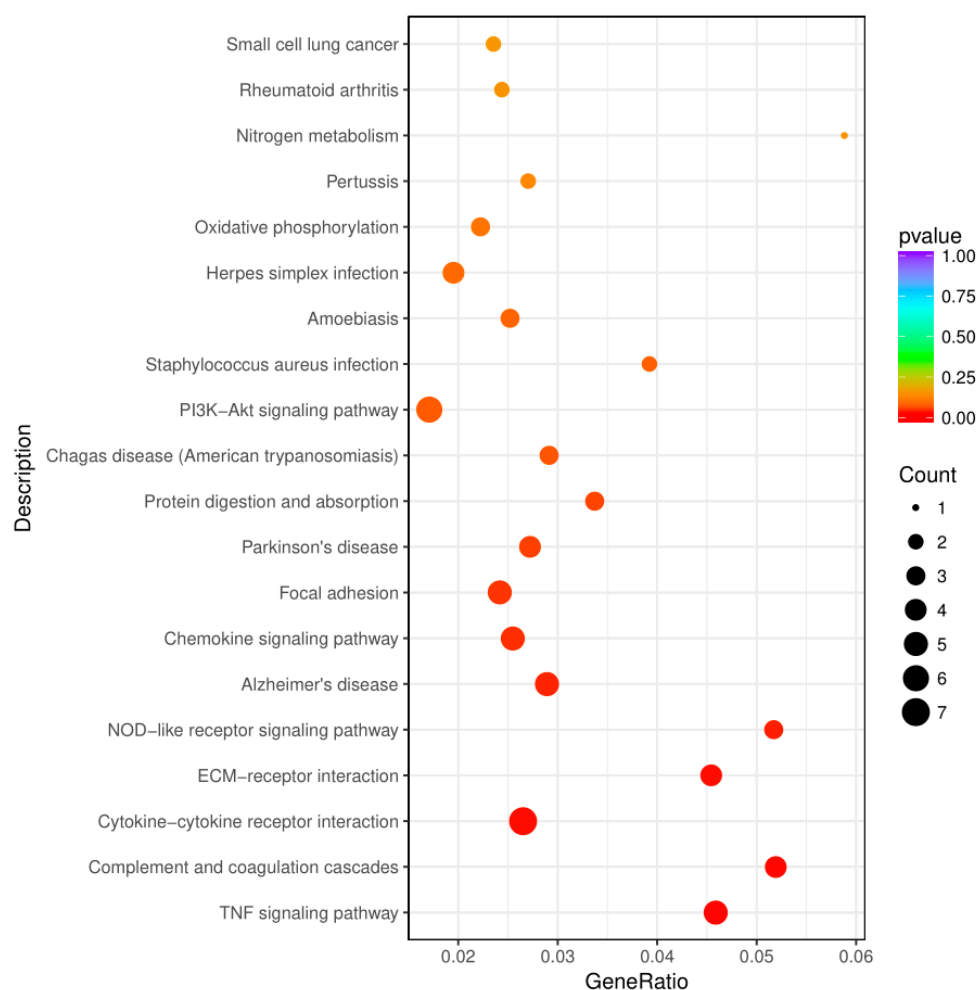


Figure 5. KEGG enrichment *p* value result graph induced by DEGs between 50 µg/mL concentrations of EYG group and control group. The ordinate was pathway name, and the abscissa was Gene Ratio. The size of dots represents the number of differentially expressed genes in this pathway, and the color of dots corresponds to different *p* value ranges.

We further explored the mechanism of several enriched pathways (Table 2) and found that EYG upregulated COL2A1, COL4A1, COL4A2 and other factors to enrich the signaling pathways. Besides, we also knew that EYG downregulated CCL2, CCL5, NOD2 and other factors to inhibit the inflammation-related pathways.

Table 2. Enrichment of KEGG pathway for DEGs between treatment with 50 µg/mL EYG and the control. *p* < 0.05 was considered statistically significant.

Pathway	ID	Gene Name	Corrected <i>p</i> -Value
UP			
ECM–receptor interaction	mmu04512	COL2A1	0.016550785
		COL4A2	
		COL4A1	
Protein digestion and absorption	mmu04974	COL2A1	0.016550785
		COL4A2	
		COL4A1	

Table 2. *Cont.*

Pathway	ID	Gene Name	Corrected <i>p</i> -Value
Focal adhesion	mmu04510	COL2A1	0.016550785
		COL4A2	
		COL4A1	
		PDGFB	
Amoebiasis	mmu05146	COL2A1	0.024727215
		COL4A2	
		COL4A1	
DOWN			
TNF signaling pathway	mmu04668	CCL5	0.028943572
		CCL2	
		NOD2	
		MMP9	
		BCL3	
Complement and coagulation cascades	mmu04610	F13a1	0.036868851
		C4b	
		Serpinf2	
		C3	

3.8. PPI (Protein–Protein Interaction) Network

The PPI network with 14 nodes and 15 interaction pairs was constructed (Figure 6). Pathway analysis showed that the complement and coagulation cascades were the most enriched signaling pathways, such as TNF signaling pathway, ECM–receptor interaction were also enriched to varying degrees.

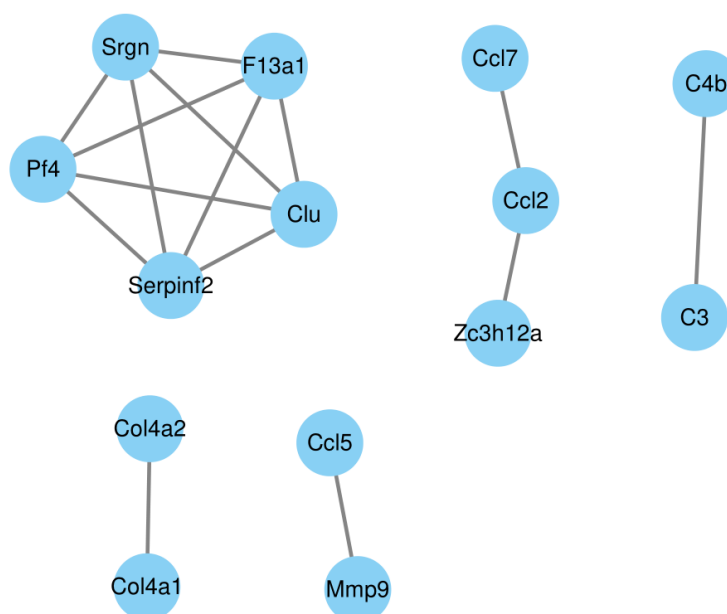


Figure 6. The PPI network of DEGs between 50 $\mu\text{g}/\text{mL}$ concentrations of EYG group and control group and its neighboring genes consisting of 14 nodes and 15 edges.

3.9. qRT-PCR Analysis

On the basis of GO analysis and KEGG analysis, PI3K-Akt signaling pathways which are the critical pathways regulating the bone formation were significantly changed in the EYG group. COL-I, BMP2, RUNX2 and β -catenin were the key regulating factor in this pathway and were selected for qRT-PCR analysis for verification of the GO analysis and KEGG analysis. The results showed that the expression of these genes in EYG-treated MC3T3-E1 cells was significantly increased in a dose-dependent manner, and the trends of qRT-PCR results were consistent with the trend of existing data analysis, which led us to propose the hypothesis that EYG affects the proliferation and differentiation of osteoblasts (Figure 7).

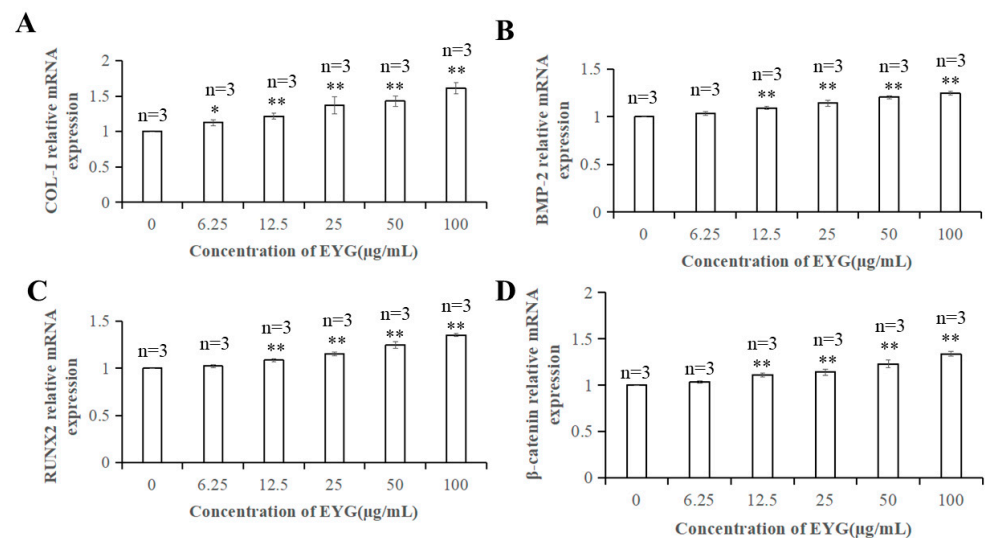


Figure 7. Gene relative expressions of COL-I (A), BMP2 (B), Runx2 (C) and β -catenin (D) by qRT-PCR analysis. MC3T3-E1 cells were treated with various concentrations of EYG. EYG significantly increased the above key factors of MC3T3-E1 osteoblast. Data were expressed as mean \pm SEM and the number of replicates was 3 ($n = 3$). Multiple comparisons were done using one way ANOVA analysis. * $p < 0.05$, ** $p < 0.01$ versus control.

4. Discussion

Recently, several studies used transcriptional profiling to address osteoblast differentiation. Some focus on gene expression profile of osteoporotic phenotype mice [41], and others used transcriptional analysis to investigate gene expression differences in osteoblast differentiation of MC3T3-E1 cells [42,43]. In this study, after we identified several common pathways and connected DEGs with potential biological pathways by transcriptome analysis, we found that EYG had an effect on several bone formation related pathways, such as TNF signaling pathway, complement and coagulation cascades, protein digestion and absorption, ECM–receptor interaction and focal adhesion.

In our study, we noticed the TNF signal pathway and complement and coagulation cascades were downregulated with the EYG treatment. It has been proved that complement and coagulation cascades are activated after bone fracture, triggering a local or systemic inflammatory response [44]. Besides, persistent inflammation can control bone mass by affecting bone formation balance, and TNF- α as one of the most potential pro-inflammatory cytokines can inhibit osteoblast differentiation and bone regeneration under the inflammatory conditions [45,46]. As for the inflammatory factors in the pathway, BCL3 and NOD2 can activate the downstream NF- κ B signaling to promote RANKL-induced osteoclastogenesis [47,48]. Modulating imbalance and dysregulation of proinflammatory mediators CCL5 can improve bone formation [49] and high expression of CCL2 is often associated with macrophage aggregation and inflammatory response [50]. On this basis, EYG may

inhibit the gene expression of osteoclasts and promote the formation of osteoblasts by downregulating inflammatory factors.

In the current study, ECM–receptor interaction, focal adhesion and protein digestion and absorption were the most significant pathways for upregulated genes. ECM, as an important component of cell microenvironment, influences cell behavior and tissue development by regulating cell adhesion, migration, apoptosis, proliferation and differentiation [51,52]. Tissue-specific and stage-specific ECM plays an important role in regulating differentiation of mesenchymal stem cells into specific cell types [53]. Focal adhesion is also closely related to osteoblastic differentiation. Laminin-5 can make focal adhesion kinase (FAK) activation regulate osteogenic differentiation of hMSCs without any soluble osteogenic supplements [54]. Moreover, transmembrane integrin heterodimers are key factors in focal adhesion pathways, connecting extracellular domains to ECM molecules such as collagen, thus playing a role in osteoblast differentiation [55].

ECM proteins include collagen and non-collagenous glycoproteins [56,57]. In addition to COL-I, there are many collagen proteins that are closely related to calcification deposition in osteoblastic differentiation. COL2A1 served as markers of the differentiation of proliferative chondrocytes [58]. COL4 is one of the main components of cellular basement membranes and COL4A1 and COL4A2 encode the $\alpha 1$, $\alpha 2$ chain of COL4. Mutations in COL4A1 and COL4A2 may lead to maladjustment of multiple systems, resulting in a variety of multifactorial diseases [59]. Microarray analysis proved that COL4A1mRNA has more expression in osteoporotic human bone than in normal human bone [60]. The signaling pathways of regulation of the focal adhesion play critical roles in regulating cell spreading by the downregulation of COL4A1 and COL4A2 in the early stage of osteoblast differentiation and COL4A1 may be a critical marker [61]. COL4A2 in the tissue-specific ECM can make Wnt/ β -catenin pathway inhibition promote osteogenic differentiation [62]. Our results showed that COL2A1, COL4A1 and COL4A2 were downregulated in the KEGG analysis, which may result from the downregulation of ECM–receptor interaction and focal adhesion. On this basis, we hypothesize that EYG may promote the related gene expression of formation of osteoblasts by regulating main components of cellular basement membranes and ECM–receptor interaction and focal adhesion to treat osteoporosis. However, the specific mechanism and connections still need further research.

5. Conclusions

EYG can influence multiple biological processes and changes in cellular composition including increasing ALP activity of MC3T3-E1 cells, promoting the secretion of extracellular matrix protein COL-I and OCN, increasing the quantity of bone mineralization calcium nodules and promoting new bone formation. Transcriptome analyses revealed the inflammation was inhibited through EYG acting on the TNF signaling pathway and complement and coagulation cascades. Besides, EYG can raise the gene expression of ECM proteins COL2A1, COL4A1 and COL4A2, which considering their known roles in osteogenesis, may explain the proliferation and differentiation observed with EYG treatment. This study provides a scientific theoretical basis for the use of EYG as a nutritional intervention food to prevent osteoporosis.

Author Contributions: S.H. and K.M. conception, design, wrote the original draft and participated in analyzing the data; M.C. performed experiments and participated in manuscript writing; L.Z., Q.X. and Z.Q. review and editing the manuscript. G.X. and X.S. obtained funding, conceived the study and finalized manuscript. All authors have read and agreed to the published version of the manuscript.

Funding: This research was funded by Hainan Provincial Natural Science Foundation of China (no. 319QN331), Innovative Research Projects of Graduate Students of Hainan Province (no. hys2019-73) and the Scientific Research Foundation of Hainan University (no. kyqd1662).

Data Availability Statement: The data presented in this study are available on request from the corresponding author.

Conflicts of Interest: The authors declare no conflict of interest.

References

1. Cummings, S.R.; Black, D. Bone mass measurements and risk of fracture in caucasian women: A review of findings from prospective studies. *Am. J. Med.* **1995**, *98*, 24S–28S. [[CrossRef](#)]
2. Wirries, A.; Schubert, A.K.; Zimmermann, R.; Jabari, S.; Ruchholtz, S.; El-Najjar, N. Thymoquinone accelerates osteoblast differentiation and activates bone morphogenetic protein-2 and ERK pathway. *Int. Immunopharmacol.* **2013**, *15*, 381–386. [[CrossRef](#)]
3. Zhang, X.Y.; Xue, Y.; Zhang, Y.J.B. Effects of 0.4 T rotating magnetic field exposure on density, strength, calcium and metabolism of rat thigh bones. *Bioelectromagnetics* **2010**, *27*, 1–9. [[CrossRef](#)] [[PubMed](#)]
4. Katagiri, T.; Takahashi, N. Regulatory mechanisms of osteoblast and osteoclast differentiation. *Oral Dis.* **2010**, *8*, 147–159. [[CrossRef](#)] [[PubMed](#)]
5. Uehara, K.; Takahashi, A.; Watanabe, M.; Nomura, Y. Shark protein improves bone mineral density in ovariectomized rats and inhibits osteoclast differentiation. *Nutrition* **2014**, *30*, 719–725. [[CrossRef](#)]
6. Xie, C.-L.; Park, K.H.; Kang, S.S.; Cho, K.M.; Lee, D.H. Isoflavone-enriched soybean leaves attenuate ovariectomy-induced osteoporosis in rats by anti-inflammatory activity. *J. Sci. Food Agric.* **2021**, *101*, 1499–1506. [[CrossRef](#)]
7. Fu, M.; Tian, Y.; Zhang, T.; Zhan, Q.; Zhang, L.; Wang, J. Comparative study of DHA-enriched phosphatidylcholine and EPA-enriched phosphatidylcholine on ameliorating high bone turnover via regulation of the osteogenesis-related Wnt/ β -catenin pathway in ovariectomized mice. *Food Funct.* **2020**, *11*, 10094–10104. [[CrossRef](#)]
8. Mei, F.; Meng, K.; Gu, Z.; Yun, Y.; Zhang, W.; Zhang, C.; Zhong, Q.; Pan, F.; Shen, X.; Xia, G.; et al. Arecanut (*Areca catechu* L.) Seed Polyphenol-Ameliorated Osteoporosis by Altering Gut Microbiome via LYZ and the Immune System in Estrogen-Deficient Rats. *J. Agric. Food Chem.* **2021**, *69*, 246–258. [[CrossRef](#)]
9. Xia, G.; Wang, J.; Sun, S.; Zhao, Y.; Wang, Y.; Yu, Z.; Wang, S.; Xue, C. Sialoglycoproteins prepared from the eggs of *Carassius auratus* prevent bone loss by inhibiting the NF- κ B pathway in ovariectomized rats. *Food Funct.* **2016**, *7*, 704–712. [[CrossRef](#)]
10. Xia, G.; Yu, Z.; Zhao, Y.; Wang, Y.; Wang, S.; He, M.; Wang, J.; Xue, C. Sialoglycoproteins isolated from the eggs of *Carassius auratus* prevents osteoporosis by suppressing the activation of osteoclastogenesis related NF- κ B and MAPK pathways. *J. Funct. Foods* **2015**, *17*, 491–503. [[CrossRef](#)]
11. Xia, G.; Zhao, Y.; Yu, Z.; Tian, Y.; Wang, Y.; Wang, S.; Wang, J.; Xue, C. Phosphorylated Peptides from Antarctic Krill (*Euphausia superba*) Prevent Estrogen Deficiency Induced Osteoporosis by Inhibiting Bone Resorption in Ovariectomized Rats. *J. Agric. Food Chem.* **2015**, *63*, 9550–9557. [[CrossRef](#)]
12. Canalis, E.; Economides, A.N.; Gazzerro, E. Bone morphogenetic proteins, their antagonists, and the skeleton. *Endocr. Rev.* **2003**, *24*, 218–235. [[CrossRef](#)] [[PubMed](#)]
13. Stein, G.S.; Lian, J.B. Molecular Mechanisms Mediating Proliferation/Differentiation Interrelationships During Progressive Development of the Osteoblast Phenotype. *Endocr. Rev.* **1993**, *14*, 424–442. [[CrossRef](#)] [[PubMed](#)]
14. Blair, H.C.; Larrouture, Q.C.; Li, Y.; Lin, H.; Beer-Stoltz, D.; Liu, L.; Tuan, R.S.; Robinson, L.J.; Schlesinger, P.H.; Nelson, D.J. Osteoblast Differentiation and Bone Matrix Formation In Vivo and In Vitro. *Tissue Eng. Part B Rev.* **2017**, *23*, 268–280. [[CrossRef](#)]
15. Carvalho, M.S.; Poundarik, A.A.; Cabral, J.M.S.; da Silva, C.L.; Vashishth, D. Biomimetic matrices for rapidly forming mineralized bone tissue based on stem cell-mediated osteogenesis. *Sci. Rep.* **2018**, *8*, 14388. [[CrossRef](#)]
16. Komori, T. Regulation of osteoblast differentiation by transcription factors. *J. Cell. Biochem.* **2010**, *99*, 1233–1239. [[CrossRef](#)]
17. Tarkkonen, K.; Hieta, R.; Kytölä, V.; Nykter, M.; Kiviranta, R. Comparative analysis of osteoblast gene expression profiles and Runx2 genomic occupancy of mouse and human osteoblasts in vitro. *Gene* **2017**, *626*, 119–131. [[CrossRef](#)] [[PubMed](#)]
18. Byers, B.A.; García, A.J. Exogenous Runx2 Expression Enhances In Vitro Osteoblastic Differentiation and Mineralization in Primary Bone Marrow Stromal Cells. *Tissue Eng.* **2004**, *10*, 1623–1632. [[CrossRef](#)]
19. Visser, R.; Bodnarova, K.; Arrabal, P.M.; Cifuentes, M.; Becerra, J. Combining bone morphogenetic proteins-2 and -6 has additive effects on osteoblastic differentiation in vitro and accelerates bone formation in vivo. *J. Biomed. Mater. Res. Part A* **2015**, *104*, 178–185. [[CrossRef](#)]
20. Dijke, P.T. Bone morphogenetic protein signal transduction in bone. *Curr. Med. Res. Opin.* **2006**, *22*, S7–S11. [[CrossRef](#)]
21. Miyazono, K.; Maeda, S.; Imamura, T. BMP receptor signaling: Transcriptional targets, regulation of signals, and signaling cross-talk. *Cytokine Growth Factor Rev.* **2005**, *16*, 251–263. [[CrossRef](#)]
22. Martín-Millán, M.; González-Martín, M.C.; Ruiz, P.; Almeida, M.; Ros, M.A.; González-Macías, J. La vía Wnt/ β -catenina disminuye la cantidad de osteoclastos en el hueso y favorece su apoptosis. *Rev. Osteoporos. Metab. Miner.* **2019**, *11*, 39–45. [[CrossRef](#)]
23. Galli, C.; Piemontese, M.; Lumetti, S.; Manfredi, E.; Passeri, G. GSK3b-inhibitor lithium chloride enhances activation of Wnt canonical signaling and osteoblast differentiation on hydrophilic titanium surfaces. *Clin. Oral Implant. Res.* **2013**, *24*, 921–927. [[CrossRef](#)]
24. Glass, D.A., 2nd; Bialek, P.; Ahn, J.D.; Starbuck, M.; Patel, M.S.; Clevers, H.; Taketo, M.M.; Long, F.; McMahon, A.P.; Lang, R.A.; et al. Canonical Wnt signaling in differentiated osteoblasts controls osteoclast differentiation. *Dev. Cell* **2005**, *8*, 751–764. [[CrossRef](#)] [[PubMed](#)]

25. Dong, J.; Xu, X.; Zhang, Q.; Yuan, Z.; Tan, B. The PI3K/AKT pathway promotes fracture healing through its crosstalk with Wnt/ β -catenin. *Exp. Cell Res.* **2020**, *394*, 112137. [[CrossRef](#)]
26. Kim, H.K.; Lee, S.; Leem, K.H. Protective effect of egg yolk peptide on bone metabolism. *Menopause N. Y.* **2011**, *18*, 307–313. [[CrossRef](#)]
27. Xia, G.; Wang, S.; He, M.; Zhou, X.; Zhao, Y.; Wang, J.; Xue, C. Anti-osteoporotic activity of sialoglycoproteins isolated from the eggs of *Carassius auratus* by promoting osteogenesis and increasing OPG/RANKL ratio. *J. Funct. Foods* **2015**, *15*, 137–150. [[CrossRef](#)]
28. Zhan, Q.; Dai, Y.; Wang, F.; Mai, X.; Wang, J. Metabonomic analysis in investigating the anti-osteoporotic effect of sialoglycoprotein isolated from eggs of *carassius auratus* on ovariectomized mice. *J. Funct. Foods* **2019**, *61*, 103514. [[CrossRef](#)]
29. Seko, A.; Koketsu, M.; Nishizono, M.; Enoki, Y.; Ibrahim, H.R.; Juneja, L.R.; Kim, M.; Yamamoto, T. Occurrence of a sialylglycopeptide and free sialylglycans in hen's egg yolk. *Biochim. Biophys. Acta Gen. Subj.* **1997**, *1335*, 23–32. [[CrossRef](#)]
30. Zou, Y.; Wu, Z.; Chen, L.; Liu, X.; Gu, G.; Xue, M.; Wang, P.G.; Chen, M. An Efficient Approach for Large-Scale Production of Sialylglycopeptides from Egg Yolks. *J. Carbohydr. Chem.* **2012**, *31*, 436–446. [[CrossRef](#)]
31. Kobayashi, T.; Koie, H.; Watanabe, A.; Ino, A.; Watabe, K.; Kim, M.; Kanayama, K.; Otsuji, K. Effects of food enriched with egg yolk hydrolysate (bone peptide) on bone metabolism in orchidectomized dogs. *J. Vet. Med. Sci.* **2015**, *77*, 503–506. [[CrossRef](#)]
32. Leem, K.H.; Kim, M.G.; Kim, H.M.; Kim, M.; Lee, Y.J.; Kim, H.K. Effects of Egg Yolk Proteins on the Longitudinal Bone Growth of Adolescent Male Rats. *Biosci. Biotechnol. Biochem.* **2004**, *68*, 2388–2390. [[CrossRef](#)]
33. Ji, M.; Leem, K.-H.; Kim, M.; Kim, H.K. Egg yolk soluble protein stimulates the proliferation and differentiation of osteoblastic MC3T3-E1 cells. *Biosci. Biotechnol. Biochem.* **2007**, *71*, 1327–1329. [[CrossRef](#)]
34. Sun, B.; Bao, W.; Tian, X.; Li, M.; Liu, H.; Dong, J.; Huang, W. A simplified procedure for gram-scale production of sialylglycopeptide (SGP) from egg yolks and subsequent semi-synthesis of Man3GlcNAc oxazoline. *Carbohydr. Res.* **2014**, *396*, 62–69. [[CrossRef](#)]
35. Liu, L.; Prudden, A.R.; Bosman, G.P.; Boons, G.J. Improved isolation and characterization procedure of sialylglycopeptide from egg yolk powder. *Carbohydr. Res.* **2017**, *452*, 122–128. [[CrossRef](#)] [[PubMed](#)]
36. Mei, F.; Liu, J.; Wu, J.; Duan, Z.; Chen, M.; Meng, K.; Chen, S.; Shen, X.; Xia, G.; Zhao, M. Collagen Peptides Isolated from *Salmo salar* and *Tilapia nilotica* Skin Accelerate Wound Healing by Altering Cutaneous Microbiome Colonization via Upregulated NOD2 and BD14. *J. Agric. Food Chem.* **2020**, *68*, 1621–1633. [[CrossRef](#)] [[PubMed](#)]
37. Jiang, S.; Zeng, M.; Zhao, Y. Thermal processed *Crassostrea gigas* impact the mouse gut microbiota. *J. Funct. Foods* **2020**, *75*, 104254. [[CrossRef](#)]
38. Wang, W.; Olson, D.; Cheng, B.; Guo, X.; Wang, K. Sanguis Draconis resin stimulates osteoblast alkaline phosphatase activity and mineralization in MC3T3-E1 cells. *J. Ethnopharmacol.* **2012**, *142*, 168–174. [[CrossRef](#)] [[PubMed](#)]
39. Li, F.; Yang, Y.; Zhu, P.; Chen, W.; Qi, D.; Shi, X.; Zhang, C.; Yang, Z.; Li, P. Echinacoside promotes bone regeneration by increasing OPG/RANKL ratio in MC3T3-E1 cells. *Fitoterapia* **2012**, *83*, 1443–1450. [[CrossRef](#)]
40. Park, K.; Ju, W.C.; Yeo, J.H.; Kim, J.Y.; Seo, H.S.; Uchida, Y.; Cho, Y. Increased OPG/RANKL ratio in the conditioned medium of soybean-treated osteoblasts suppresses RANKL-induced osteoclast differentiation. *Int. J. Mol. Med.* **2014**, *33*, 178–184. [[CrossRef](#)]
41. Wang, C.; Yu, T.; Tan, L.; Cheng, J. Bioinformatics analysis of gene expression profile in callus tissues of osteoporotic phenotype mice induced by osteoblast-specific *Krm2* overexpression. *Int. J. Rheum. Dis.* **2016**, *19*, 1263–1271. [[CrossRef](#)] [[PubMed](#)]
42. Yuan, Y.; Duan, R.; Wu, B.; Huang, W.; Zhang, X.; Qu, M.; Liu, T.; Yu, X. Gene expression profiles and bioinformatics analysis of insulin-like growth factor-1 promotion of osteogenic differentiation. *Mol. Genet. Genom. Med.* **2019**, *7*, e00921. [[CrossRef](#)] [[PubMed](#)]
43. Liu, Y.; Wang, H.; Zhou, X.-Z.; Li, N.; Guo, Y.-C.; Chen, T.-P. Pentraxin 3 promotes the osteoblastic differentiation of MC3T3-E1 cells through the PI3K/Akt signaling pathway. *Biosci. Rep.* **2020**, *40*. [[CrossRef](#)] [[PubMed](#)]
44. Huber-Lang, M.; Ignatius, A.; Brenner, R.E. Role of Complement on Broken Surfaces After Trauma. *Adv. Exp. Med. Biol.* **2015**, *865*, 43–55.
45. Xu, C.P.; Li, X.; Hu, Y.J.; Cui, Z.; Wang, L.; Liang, L.; Zhou, Y.L.; Yang, Y.J.; Yu, B. Quantitative proteomics reveals ELP2 as a regulator to the inhibitory effect of TNF- α on osteoblast differentiation. *J. Proteom.* **2015**, *114*, 234–246. [[CrossRef](#)] [[PubMed](#)]
46. Jeong, B.-C. ATF3 mediates the inhibitory action of TNF- α on osteoblast differentiation through the JNK signaling pathway. *Biochem. Biophys. Res. Commun.* **2018**, *499*, 696–701. [[CrossRef](#)]
47. Ke, K.; Sul, O.; Chung, S.; Suh, J.; Choi, H.S. Lack of NOD2 attenuates ovariectomy-induced bone loss via inhibition of osteoclasts. *J. Endocrinol.* **2017**, *235*, 85–96. [[CrossRef](#)]
48. Wang, K.; Li, S.; Gao, Y.; Feng, X.; Liu, W.; Luo, R.; Song, Y.; Tu, J.; Liu, Y.; Yang, C. BCL3 regulates RANKL-induced osteoclastogenesis by interacting with TRAF6 in bone marrow-derived macrophages. *Bone* **2018**, *114*, 257–267. [[CrossRef](#)]
49. Hong, L.; Sharp, T.; Khorsand, B.; Fischer, C.; Amendt, B.A. MicroRNA-200c Represses IL-6, IL-8, and CCL-5 Expression and Enhances Osteogenic Differentiation. *PLoS ONE* **2016**, *11*, e0160915.
50. Lin, S.K.; Chang, H.H.; Chen, Y.J.; Wang, C.C.; Galson, D.L.; Hong, C.Y.; Kok, S.H. Epigallocatechin-3-gallate diminishes CCL2 expression in human osteoblastic cells via up-regulation of phosphatidylinositol 3-Kinase/Akt/Raf-1 interaction: A potential therapeutic benefit for arthritis. *Arthritis Rheum.* **2010**, *58*, 3145–3156. [[CrossRef](#)]
51. Mathews, S.; Bhonde, R.; Gupta, P.K.; Totey, S. Extracellular matrix protein mediated regulation of the osteoblast differentiation of bone marrow derived human mesenchymal stem cells. *Differentiation* **2012**, *84*, 185–192. [[CrossRef](#)]

52. Ventura, R.D.; Padalhin, A.R.; Kim, B.; Park, M.K.; Lee, B.T. Evaluation of bone regeneration potential of injectable extracellular matrix (ECM) from porcine dermis loaded with biphasic calcium phosphate (BCP) powder. *Mater. Sci. Eng. C* **2020**, *110*, 110663. [[CrossRef](#)]
53. Hoshiba, T.; Kawazoe, N.; Chen, G. The balance of osteogenic and adipogenic differentiation in human mesenchymal stem cells by matrices that mimic stepwise tissue development. *Biomaterials* **2012**, *33*, 2025–2031. [[CrossRef](#)] [[PubMed](#)]
54. Klees, R.F.; Salaszyk, R.M.; Vandenberg, S.; Bennett, K.; Plopper, G.E. Laminin-5 activates extracellular matrix production and osteogenic gene focusing in human mesenchymal stem cells. *Matrix Biol.* **2007**, *26*, 106–114. [[CrossRef](#)]
55. Castillo, A.B. Focal Adhesion Kinase Plays a Role in Osteoblast Mechanotransduction In Vitro but Does Not Affect Load- Induced Bone Formation In Vivo. *PLoS ONE* **2012**. [[CrossRef](#)] [[PubMed](#)]
56. Licini, C.; Vitale-Brovarone, C.; Mattioli-Belmonte, M. Collagen and non-collagenous proteins molecular crosstalk in the pathophysiology of osteoporosis. *Cytokine Growth Factor Rev.* **2019**, *49*, 59–69. [[CrossRef](#)] [[PubMed](#)]
57. Carvalho, M.S.; Cabral, J.M.S.; da Silva, C.L.; Vashishth, D. Bone Matrix Non-Collagenous Proteins in Tissue Engineering: Creating New Bone by Mimicking the Extracellular Matrix. *Polymer* **2021**, *13*, 1095. [[CrossRef](#)]
58. Paradis, F.-H.; Hales, B.F. The Effects of Class-Specific Histone Deacetylase Inhibitors on the Development of Limbs During Organogenesis. *Toxicol. Ences Off. J. Soc. Toxicol.* **2015**, *148*, 220–228. [[CrossRef](#)] [[PubMed](#)]
59. Jeanne, M.; Gould, D.B. Genotype-phenotype correlations in pathology caused by collagen type IV alpha 1 and 2 mutations. *Matrix Biol.* **2016**, *57*, 29–44. [[CrossRef](#)]
60. Hopwood, B. Gene expression profile of the bone microenvironment in human fragility fracture bone. *Bone* **2009**, *44*, 87–101. [[CrossRef](#)]
61. Dun, H. Morphological and proteomic analysis of early stage of osteoblast differentiation in osteoblastic progenitor cells. *Exp. Cell Res.* **2010**, *316*, 2291–2300.
62. Wen, Y.; Yang, H.; Wu, J.; Wang, A.; Jin, Z. COL4A2 in the tissue-specific extracellular matrix plays important role on osteogenic differentiation of periodontal ligament stem cells. *Theranostics* **2019**, *9*, 4265–4286. [[CrossRef](#)] [[PubMed](#)]